

Journal of Materials Chemistry A

Accepted Manuscript



This is an *Accepted Manuscript*, which has been through the Royal Society of Chemistry peer review process and has been accepted for publication.

Accepted Manuscripts are published online shortly after acceptance, before technical editing, formatting and proof reading. Using this free service, authors can make their results available to the community, in citable form, before we publish the edited article. We will replace this *Accepted Manuscript* with the edited and formatted *Advance Article* as soon as it is available.

You can find more information about *Accepted Manuscripts* in the [Information for Authors](#).

Please note that technical editing may introduce minor changes to the text and/or graphics, which may alter content. The journal's standard [Terms & Conditions](#) and the [Ethical guidelines](#) still apply. In no event shall the Royal Society of Chemistry be held responsible for any errors or omissions in this *Accepted Manuscript* or any consequences arising from the use of any information it contains.

Impact of lithium excess on the structural and electrochemical properties of $\text{LiNi}_{0.5}\text{Mn}_{1.5}\text{O}_4$ high-voltage cathode material †

Received 00th January 20xx,
Accepted 00th January 20xx

Yu-Feng Deng,^{ab} Shi-Xi Zhao,^{ab*} Peng-Yuan Zhai,^{ab} Guozhong Cao^c and Ce-Wen Nan^b

DOI: 10.1039/x0xx00000x

www.rsc.org/

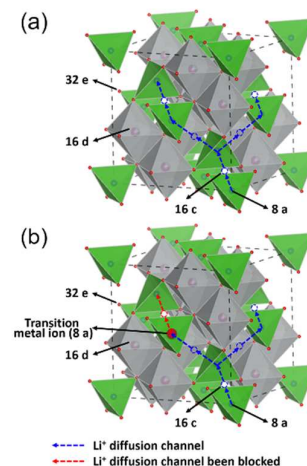
$\text{LiNi}_{0.5}\text{Mn}_{1.5}\text{O}_4$ -based cathodes materials are synthesized by one-step nonaqueous co-precipitation method. Appropriate excess lithium ions can extrude transition metal ions out of tetrahedral 8a sites, which could have a higher effect on the rate performance of $\text{LiNi}_{0.5}\text{Mn}_{1.5}\text{O}_4$ than the well-known factor, i.e. cationic order degree in 16d octahedral sites.

$\text{LiNi}_{0.5}\text{Mn}_{1.5}\text{O}_4$ is a promising cathode material for lithium-ion batteries as it offers a high operating voltage of ~ 4.7 V arising from $\text{Ni}^{2+/4+}$ couple instead of $\text{Mn}^{3+/4+}$ couple of spinel LiMn_2O_4 .^{1, 2} It possesses two similar crystal structures. One with a random distribution of Mn^{4+} and Ni^{2+} ions in the octahedral 16d sites displays the disordered phase with the space group of $Fd\bar{3}m$. Another belongs to the space group of $P4_332$ with an order arrangement of Mn^{4+} and Ni^{2+} . The real structure of $\text{LiNi}_{0.5}\text{Mn}_{1.5}\text{O}_4$ contains both two phases.³ Factors influencing the performance of $\text{LiNi}_{0.5}\text{Mn}_{1.5}\text{O}_4$ mainly reported are cationic order degree in octahedral 16d sites^{4, 5} and surface planes.^{6, 7} Generally the material with lower cationic order degree is thought to have better rate performance because of its higher Li-ion diffusion coefficient.⁸

Changing annealing conditions⁹ is a traditional way to control cationic order because Mn^{3+} derived from oxygen vacancies hinders this order degree. Whittingham et al¹⁰ prepared disordered $\text{LiNi}_{0.5}\text{Mn}_{1.5}\text{O}_4$ with high-rate capability by increasing Mn^{3+} concentration. Meanwhile some other methods such as varying Ni/Mn ratio,¹¹ doping¹² and polymer-assisted method¹³ also could be actualized to control cationic order with no need for further annealing. However a common phenomenon, namely some extent of transition metal ions (Ni^{2+} and/or Mn^{4+}) occupy in the tetrahedral

8a sites instead of original Li^+ ions, usually is overlooked. Means applied to control cationic order degree in octahedral 16d sites could even enhance this staggered arrangement.¹⁴⁻¹⁸ Though the mixing effect between lithium ions and transition ions in cathodes materials with layered structure has been proven to be unfavorable to rate ability,¹⁹ its effect on the performance of spinel $\text{LiNi}_{0.5}\text{Mn}_{1.5}\text{O}_4$ has not received enough attention.

In an attempt to clarify the role of tetrahedral 8a sites occupation, a simple method was carried out: appropriate excess lithium ions can extrude transition ions out of tetrahedral 8a sites without causing morphology and structure change but an increase of cationic order degree in 16d octahedral sites. Li excess could improve the cycle ability by suppress the Jahn-Teller effect of spinel LiMn_2O_4 , while Li_2MnO_3 derived from Li-rich for the ternary layered cathodes have a great influence on the electrochemical capability.^{20, 21} Nevertheless, impact of lithium excess on $\text{LiNi}_{0.5}\text{Mn}_{1.5}\text{O}_4$ is lack of study. Following characterizations would provide results that avoiding the transition metal ions occupation in tetrahedral 8a sites by Li excess is beneficial to mobility of Li^+ . The diffusion channel of Li^+ , 8a-16c-8a, is liable to be blocked by transition metal ions in tetrahedral 8a sites, as shown in Fig. 1.



In this work, one-step nonaqueous co-precipitation method (Fig.

Fig. 1 Schematic illustration of (a) Li^+ diffusion channel and (b) Li^+ diffusion channel been blocked in spinel $\text{LiNi}_{0.5}\text{Mn}_{1.5}\text{O}_4$ structure.

^a Graduate School at Shenzhen, Tsinghua University, Shenzhen 518055, China. E-mail: zhaosx@sz.tsinghua.edu.cn

^b School of Materials Science and Engineering, Tsinghua University, Beijing 100084, China.

^c Department of Materials Science and Engineering, University of Washington, Seattle, WA 98195, USA.

† Electronic Supplementary Information (ESI) available: Experimental details, other characterization results including SEM, particles size distribution, XPS and rate performance. See DOI: 10.1039/x0xx00000x

S1, ESI^\dagger) was applied to precipitate Li^+ , Ni^{2+} and Mn^{2+} at the same time to prepare $\text{Li}_{1+x}\text{Ni}_{0.5-x}\text{Mn}_{1.5}\text{O}_4$ ($x=0, 0.01, 0.03, 0.05$). For the reasonable comparative analysis of these two factors (tetrahedral 8a sites occupation and cationic order degree in 16d octahedral sites) influencing the rate performance, keeping identical morphologies for all samples is the prerequisite. It can be found that all the samples display regular, small octahedral grains with a size distribution of 200–500 nm. (Fig. S2, ESI^\dagger).

As shown in Fig. 2. The XRD peaks of $\text{LiNi}_{0.5}\text{Mn}_{1.5}\text{O}_4$ and $\text{Li}_{1.01}\text{Ni}_{0.49}\text{Mn}_{1.5}\text{O}_4$ coincide well with spinel structure. The lack of any superstructure diffraction peaks, which derives from the ordering of transition ions in the octahedral 16d sites, reveals that these two samples have a relatively low degree of cationic order.²² However, increasing Li amount changes the structure from disordered to ordered phase, as revealed by the existence of superstructure diffraction peaks such as (110), (210), (320) and (410) peaks.²³ It's worth noting that peaks of superstructure for $\text{Li}_{1.03}\text{Ni}_{0.47}\text{Mn}_{1.5}\text{O}_4$ are weaker than those of $\text{Li}_{1.05}\text{Ni}_{0.45}\text{Mn}_{1.5}\text{O}_4$. Of particular note, a diffraction peak appears at $2\theta \approx 30.9^\circ$, which was indexed as the (220) diffraction of the spinel compounds. The appearance of the (220) diffraction peak for $\text{Li}_{1+x}\text{Ni}_{0.5-x}\text{Mn}_{1.5}\text{O}_4$ indicates that there must be some transition metal ions occupying the tetrahedral 8a sites replacing of the original Li^+ ions.²⁴ The weak diffraction peaks marked by asterisks possibly are from $\text{Li}_2\text{Ni}_{1-y}\text{O}$.²⁵ This common impurity is only observed in $\text{LiNi}_{0.5}\text{Mn}_{1.5}\text{O}_4$ and $\text{Li}_{1.01}\text{Ni}_{0.49}\text{Mn}_{1.5}\text{O}_4$. Arrebola et al¹⁶ considered that based on the crystal field model, in spinel structure Ni^{2+} ions have a strong

XPS results show that the Mn valence state in $\text{Li}_{1+x}\text{Ni}_{0.5-x}\text{Mn}_{1.5}\text{O}_4$ is between +3 and +4, and Mn valence state increases with excess Li (Fig. S3, ESI^\dagger). The formation of oxygen vacancies could be suppressed by slow cooling process and then manganese has to take the responsibility to balance charge. In the light of spectral lines of manganese oxide, both of the manganese $2p_{3/2}$ and $2p_{1/2}$ regions can be deconvoluted into two peaks. The peaks at 642.0 and 643.3 eV of the $\text{Mn}2p_{3/2}$ spectrum arise from Mn^{3+} and Mn^{4+} ,

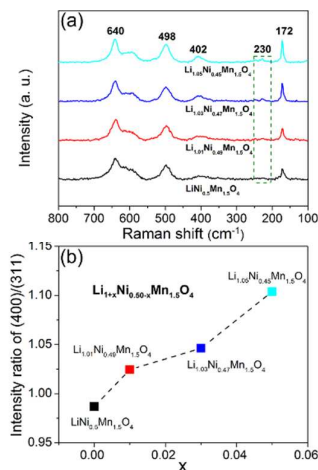


Fig. 3 (a) Raman spectra of $\text{Li}_{1+x}\text{Ni}_{0.5-x}\text{Mn}_{1.5}\text{O}_4$ samples, and (b) Intensity ratio of (400)/(311) XRD peaks.

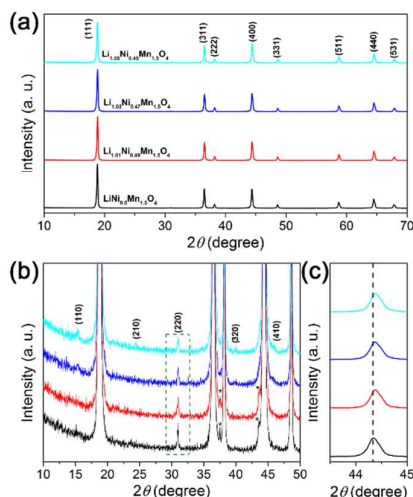


Fig. 2 XRD patterns of the four $\text{Li}_{1+x}\text{Ni}_{0.5-x}\text{Mn}_{1.5}\text{O}_4$ samples: (a) full range, (b) enlarged region to show the superstructure reflections arising from the Mn^{4+} and Ni^{2+} ordering in the 16d octahedral sites and (c) enlarged region to show the change of lattice parameter. Asterisks refer to the reflections arising from $\text{Li}_2\text{Ni}_{1-y}\text{O}$ impurity phase.

tendency to occupy octahedral 16d positions; therefore Mn was forced to occupy tetrahedral 8a positions. And the radius of Mn^{4+} (0.53 Å) is closer to Li^+ (0.59 Å) than Ni^{2+} (0.69 Å), thus it can be speculated that excess lithium ions could extrude Mn ions out of tetrahedral 8a positions to suppress the formation of Ni-rich impurity.

respectively, as are those at 653.5 eV for Mn^{3+} and 654.6 eV for Mn^{4+} in the $\text{Mn}2p_{1/2}$ spectrum.²⁶ This can explain the decrease of the lattice parameter of $\text{Li}_{1+x}\text{Ni}_{0.5-x}\text{Mn}_{1.5}\text{O}_4$ with Li substitution presented in Figure 2(c), as we know, Mn^{4+} has a smaller ionic radius ($r = 0.53 \text{ \AA}$) than Mn^{3+} ($r = 0.645 \text{ \AA}$). In like manner, Seung M. Oh et al²⁷ increased the valence state of Mn of LiMn_2O_4 . The fewer Mn^{3+} ions resulted from Li excess would bring about the higher degree of cationic order, as shown by XRD characterization.

Raman spectroscopy is a helpful testing method to determine the cationic order. According to group theory, the number of expected Raman-active modes of the ordered spinel ($6A_1+14E+22F_2$) is larger than that of the disordered spinel ($A_g+E_g+3F_{2g}$).²⁸ Figure 3(a) shows the Raman spectra of $\text{Li}_{1+x}\text{Ni}_{0.5-x}\text{Mn}_{1.5}\text{O}_4$ samples. The peaks at 640 cm^{-1} (symmetric Mn–O stretching vibration of MnO_6 groups) result from the A_g mode, the lines at 498 and 402 cm^{-1} can be assigned to the Ni^{2+} -O stretching mode in the structure. Increasing intensity of peaks at 172 and 230 cm^{-1} is characteristic of more ordered structure.¹³ It can be found that the amount of lithium increases, the degree of cationic ordering increases, which is in accord with XRD results. Besides, many researchers^{12, 15, 17, 24} used the intensity ratio of (400)/(311) of XRD pattern to estimate the distribution of transition metal ions between the 8a sites and 16d sites in spinel structure. As shown in Fig. 3(b), the intensity ratio of (400)/(311) increases as the amount of lithium increases, indicating that the amount of transition metal ions in tetrahedral 8a sites is reduced by excess lithium ions.

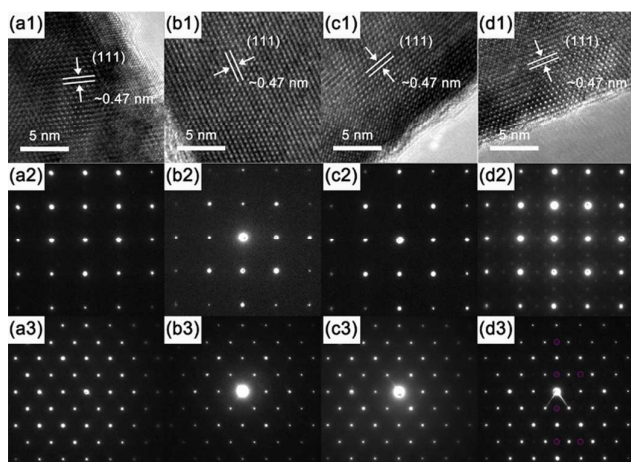


Fig. 4 HRTEM images (a1 to d1) and electron diffraction patterns in the [100] (a2 to d2) and [110] (a3 to d3) zones of (a) $\text{LiNi}_{0.5}\text{Mn}_{1.5}\text{O}_4$, (b) $\text{Li}_{1.01}\text{Ni}_{0.49}\text{Mn}_{1.5}\text{O}_4$, (c) $\text{Li}_{1.03}\text{Ni}_{0.47}\text{Mn}_{1.5}\text{O}_4$ and (d) $\text{Li}_{1.05}\text{Ni}_{0.45}\text{Mn}_{1.5}\text{O}_4$.

The high resolution electron microscopies are compared in Fig. 4 along with their diffraction patterns in the [100] and [110] zones. Fig. 4 (a1) to (d1) show the HRTEM images of the lattice fringe, of which d_{hkl} measured is ~ 0.47 nm, corresponding to the (111) interplanar distance. Only a representative spinel diffraction pattern can be observed in the [100] and [110] zones for $\text{Li}_{1+x}\text{Ni}_{0.5-x}\text{Mn}_{1.5}\text{O}_4$ ($x=0, 0.01, 0.03$), while $\text{Li}_{1.05}\text{Ni}_{0.45}\text{Mn}_{1.5}\text{O}_4$ exhibits superlattice diffraction as shown in Fig. 4 (d2 and d3).²⁹ The electron diffraction patterns show that the increasing Li amount introduces more ordered phase (or decreases disordered phase) content as well.

Galvanostatic cycling tests were conducted at a current density of $14.7 \text{ mA} \cdot \text{g}^{-1}$ (0.1 C) from 3.5 to 5.0 V, as shown in Fig. 5(a). All the cathodes exhibited two typical plateaus: long and distinct flat plateau around 4.7 V attributed to the $\text{Ni}^{2+/4+}$ redox reaction, another short plateau around 4.0 V arising from $\text{Mn}^{3+/4+}$ redox process.³⁰ The voltage plateau of 4.0 V indicates that a small number of manganese remained as Mn^{3+} ,³¹ because the oxidation state of manganese is fixed at +4 only in the ideal structure.²⁹ The length fraction of plateau at 4.0 V decreases by increasing the Li fraction. This trend can be accounted for by considering that an increase in Li amount results in a decrease of Mn^{3+} concentration, in accord with the XRD, XPS and TEM. Besides, it is worth noting that the charge plateau of $\text{LiNi}_{0.5}\text{Mn}_{1.5}\text{O}_4$ and $\text{Li}_{1.01}\text{Ni}_{0.49}\text{Mn}_{1.5}\text{O}_4$ samples around 4.7 V splitting to two plateaus corresponding to $\text{Ni}^{4+/3+}$ and $\text{Ni}^{3+/2+}$ couples individually in Fig. 5(a), while these two plateaus overlapped for $\text{Li}_{1.03}\text{Ni}_{0.47}\text{Mn}_{1.5}\text{O}_4$ and $\text{Li}_{1.05}\text{Ni}_{0.45}\text{Mn}_{1.5}\text{O}_4$. It has been reported that the narrower separation between the two voltage plateaus indicating a higher degree of cationic ordering.³² A more detailed analysis is further possible with the dQ/dV plots (Q = specific capacity and V = voltage). The two dQ/dV peaks in the 4.7 V region indicate respectively the two-step oxidation or reduction for the $\text{Ni}^{4+/2+}$ redox couple. The inset of Fig. 5(b) is the dQ/dV plots in 4V region of the spinel cathodes, also showing that the intensity of peak in the 4.0 V regions reduces by increasing the Li fraction.

In order to study the effect of excess lithium on diffusion of Li^+ in the cathodes, the electrochemical impedance spectroscopy was

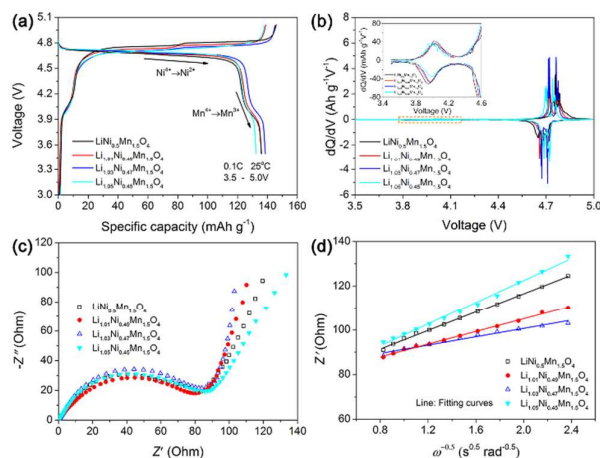


Fig. 5 (a) Charge and discharge profiles, (b) dQ/dV versus voltage in 4-V region, (c) EIS spectra at 25 °C before cycling and (d) Z_{re} vs. $\omega^{-0.5}$ plots in the low-frequency region obtained from EIS measurements of the four $\text{Li}_{1+x}\text{Ni}_{0.5-x}\text{Mn}_{1.5}\text{O}_4$ samples.

performed. Fig. 5(c) displays the Nyquist plots of the spinel electrodes before cycling. All EIS contain one semicircle in the high- and medium-frequency regions and an inclined line in the low frequency zone. The diffusion coefficient (D_{Li}) of lithium ion can be calculated from the plots in the low-frequency region using the equation³³:

$$D_{\text{Li}} = \frac{(RT)^2}{2(A n^2 F^2 C_{\text{Li}} \sigma^2)}$$

where the implications of T is the kelvin degree, R the universal gas constant, n the number of electrons per molecule during reaction, A the superficial area, F the Faraday's constant, C_{Li} the lithium ion concentration, ω the angular frequency, and σ is the Warburg factor. The $Z_{re}-\omega^{-0.5}$ plots to calculate σ is presented in Fig. 5(d). A linear characteristic could be seen for both profiles. The calculated lithium ion diffusion coefficient of $\text{Li}_{1.03}\text{Ni}_{0.47}\text{Mn}_{1.5}\text{O}_4$ is higher than other three samples, which is calculated as $3.159 \times 10^{-10} \text{ cm}^2 \text{ s}^{-1}$ and close to that measured by CV.³⁴ Interestingly, though $\text{Li}_{1.03}\text{Ni}_{0.47}\text{Mn}_{1.5}\text{O}_4$ exhibits higher degree of cationic ordering than $\text{LiNi}_{0.5}\text{Mn}_{1.5}\text{O}_4$ and $\text{Li}_{1.01}\text{Ni}_{0.49}\text{Mn}_{1.5}\text{O}_4$, it exhibits better lithium ion diffusion capability, implying that well-known factor, cationic order degree in 16d octahedral sites, does not dominates the Li^+ transport for these three samples.

The cycle and rate performances (Fig. 6) are in good agreement with EIS results. At 25 °C, the $\text{LiNi}_{0.5}\text{Mn}_{1.5}\text{O}_4$, $\text{Li}_{1.01}\text{Ni}_{0.49}\text{Mn}_{1.5}\text{O}_4$, $\text{Li}_{1.03}\text{Ni}_{0.47}\text{Mn}_{1.5}\text{O}_4$ and $\text{Li}_{1.05}\text{Ni}_{0.45}\text{Mn}_{1.5}\text{O}_4$ samples delivered initial specific capacities of 105.9, 114.8, 123.7 and 88.1 $\text{mAh} \cdot \text{g}^{-1}$ at a 5 C rate and retained 93.4%, 95.0%, 95.7% and 96.0% after 300 cycles, respectively. It can be seen that the coulombic efficiency of the initial cycle for all the samples is relatively low because the batteries were charged at 0.1C, and then discharged at 5 C, but it became higher and stable in the following cycles. The Li-excess samples exhibited higher coulombic efficiency resulting in better cycle performance. The cycle ability is comparable with $\text{LiNi}_{0.5}\text{Mn}_{1.5}\text{O}_4$ nanotubes synthesized by self-templating method, which delivered a discharge capacity of $85 \text{ mAh} \cdot \text{g}^{-1}$ at 5 C even after 550 cycles.³⁵ At a high rate of 30 C, the discharge capacity of $\text{Li}_{1.03}\text{Ni}_{0.47}\text{Mn}_{1.5}\text{O}_4$ can still reach $90.1 \text{ mAh} \cdot \text{g}^{-1}$, corresponding to

72.8% of its capacity at 1 C. It is important to note that the discharge specific capacity at high C-rates was significantly improved for $\text{Li}_{1.03}\text{Ni}_{0.47}\text{Mn}_{1.5}\text{O}_4$ compared with other samples. The $\text{Li}_{1.03}\text{Ni}_{0.47}\text{Mn}_{1.5}\text{O}_4$ electrode displays a discharge capacity of 114.2 mAh g^{-1} at 10C-rates. In contrast, the rate behaviour of $\text{Li}_{1.05}\text{Ni}_{0.45}\text{Mn}_{1.5}\text{O}_4$ worsen dramatically, it presents a discharge capacity of only 87.3 mAh g^{-1} when the current density increases to 10C.

Many researchers have reported that high degree of cationic ordering would deteriorate rate performance for its limited lithium diffusion.³⁶ In this study, the $\text{Li}_{1.05}\text{Ni}_{0.45}\text{Mn}_{1.5}\text{O}_4$ electrode with the

diffusion channel unobstructed. However, when the lithium excess is too much, it will result in obvious enhancement of the order degree in octahedral 16d sites, which is widely accepted as a negative factor for the rate capacity.

This work was supported by the National Natural Science Foundation of China (51172124, 51372136) and Shenzhen Basic Research Project (No. JCYJ20130402145002372).

Notes and references

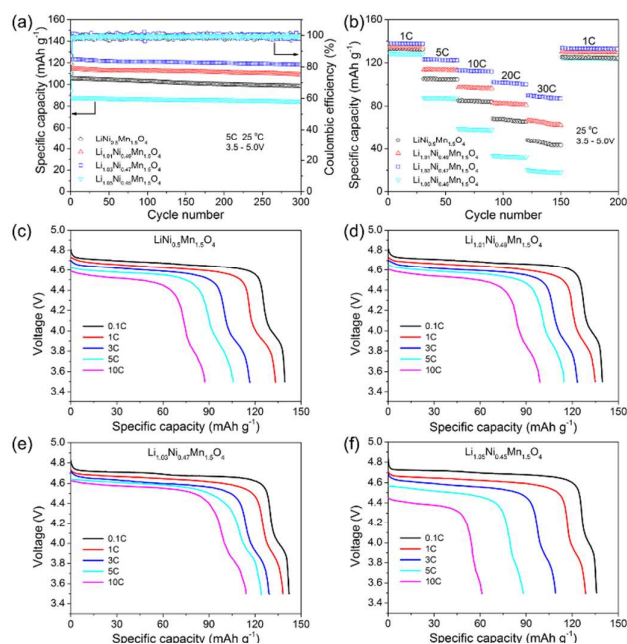


Fig. 6 Cycling stability of $\text{Li}_{1+x}\text{Ni}_{0.5-x}\text{Mn}_{1.5}\text{O}_4$ electrodes at (a) 5C rate and (b) various rates (1C, 5C, 10C, 20C, 30C); Discharge profiles of (c) $\text{LiNi}_{0.5}\text{Mn}_{1.5}\text{O}_4$, (d) $\text{Li}_{1.01}\text{Ni}_{0.49}\text{Mn}_{1.5}\text{O}_4$, (e) $\text{Li}_{1.03}\text{Ni}_{0.47}\text{Mn}_{1.5}\text{O}_4$ and (f) $\text{Li}_{1.05}\text{Ni}_{0.45}\text{Mn}_{1.5}\text{O}_4$.

highest order degree indeed shows the worst rate capability. Compared rate ability of $\text{Li}_{1.03}\text{Ni}_{0.47}\text{Mn}_{1.5}\text{O}_4$ to $\text{Li}_{1.05}\text{Ni}_{0.45}\text{Mn}_{1.5}\text{O}_4$, it can be found that $\text{Li}_{1.05}\text{Ni}_{0.45}\text{Mn}_{1.5}\text{O}_4$ with higher degree of cationic ordering delivers lower rate ability. This could because degree of cations ordering play a leading role for this two samples, in agreement with the general view.³⁷ However, for the first three samples ($\text{LiNi}_{0.5}\text{Mn}_{1.5}\text{O}_4$, $\text{Li}_{1.01}\text{Ni}_{0.49}\text{Mn}_{1.5}\text{O}_4$, $\text{Li}_{1.03}\text{Ni}_{0.47}\text{Mn}_{1.5}\text{O}_4$), excess lithium improved the rate ability obviously, indicating the transport of lithium ions could be enhanced by unhindered diffusion channel even with a more ordered arrangement of nickel and manganese ions in 16d octahedral sites.

In conclusion, octahedral grains of $\text{LiNi}_{0.5}\text{Mn}_{1.5}\text{O}_4$ -based materials are synthesized through a one-step co-precipitation method. A series of samples with increasing degree of cationic ordering in 16d octahedral sites (harmful to mobility of Li^+) were prepared, of which the amount of transition metal ions in tetrahedral 8a sites reduces (beneficial for Li^+ diffusion). The improved performance of $\text{Li}_{1.03}\text{Ni}_{0.47}\text{Mn}_{1.5}\text{O}_4$ might be attributed to appropriate excess lithium ions can preferentially occupy the tetrahedral 8a sites, extruding transition metal ions out of tetrahedral 8a positions to keep Li^+ ions

1. P. Y. Hou, J. Wang, J. S. Song, D. W. Song, X. X. Shi, X. Q. Wang and L. Q. Zhang, *Chem Commun*, 2015, 51, 3231-3234.
2. R. R. Liu, X. Deng, X. R. Liu, H. J. Yan, A. M. Cao and D. Wang, *Chem Commun*, 2014, 50, 15756-15759.
3. K. Zhang, X. P. Han, Z. Hu, X. L. Zhang, Z. L. Tao and J. Chen, *Chem Soc Rev*, 2015, 44, 699-728.
4. E. S. Lee, K. W. Nam, E. Y. Hu and A. Manthiram, *Chem Mater*, 2012, 24, 3610-3620.
5. K. M. Shaju and P. G. Bruce, *Dalton T*, 2008, DOI: 10.1039/B806662k, 5471-5475.
6. K. R. Chemelewski, D. W. Shin, W. Li and A. Manthiram, *J Mater Chem A*, 2013, 1, 3347-3354.
7. B. Hai, A. K. Shukla, H. Duncan and G. Y. Chen, *J Mater Chem A*, 2013, 1, 759-769.
8. H. F. Deng, P. Nie, L. F. Shen, H. F. Luo and X. G. Zhang, *Prog Chem*, 2014, 26, 939-949.
9. L. P. Wang, H. Li, X. J. Huang and E. Baudrin, *Solid State Ionics*, 2011, 193, 32-38.
10. J. Xiao, X. L. Chen, P. V. Sushko, M. L. Sushko, L. Kovarik, J. J. Feng, Z. Q. Deng, J. M. Zheng, G. L. Graff, Z. M. Nie, D. W. Choi, J. Liu, J. G. Zhang and M. S. Whittingham, *Adv Mater*, 2012, 24, 2109-2116.
11. J. Song, D. W. Shin, Y. H. Lu, C. D. Amos, A. Manthiram and J. B. Goodenough, *Chem Mater*, 2012, 24, 3101-3109.
12. H. L. Wang, T. A. Tan, P. Yang, M. O. Lai and L. Lui, *J Phys Chem C*, 2011, 115, 6102-6110.
13. X. L. Zhang, F. Y. Cheng, K. Zhang, Y. L. Liang, S. Q. Yang, J. Liang and J. Chen, *Rsc Adv*, 2012, 2, 5669-5675.
14. K. Amine, H. Tukamoto, H. Yasuda and Y. Fujita, *J Power Sources*, 1997, 68, 604-608.
15. T. Ohzuku, K. Ariyoshi, S. Takeda and Y. Sakai, *Electrochim Acta*, 2001, 46, 2327-2336.
16. J. C. Arrebola, A. Caballero, M. Cruz, L. Hernan, J. Morales and E. R. Castellon, *Adv Funct Mater*, 2006, 16, 1904-1912.
17. T. F. Yi, C. Y. Li, Y. R. Zhu, J. Shu and R. S. Zhu, *J Solid State Electr*, 2009, 13, 913-919.
18. H. L. Wang, H. Xia, M. O. Lai and L. Lu, *Electrochem Commun*, 2009, 11, 1539-1542.
19. Y. Cho, S. Lee, Y. Lee, T. Hong and J. Cho, *Adv Energy Mater*, 2011, 1, 821-828.
20. S. Taminato, M. Hirayama, K. Suzuki, N. L. Yamada, M. Yonemura, J. Y. Son and R. Kanno, *Chem Commun*, 2015, 51, 1673-1676.
21. S. Komaba, N. Kumagai, T. Sasaki and Y. Miki, *Electrochemistry*, 2001, 69, 784-787.
22. F. G. B. Ooms, E. M. Kelder, J. Schoonman, M. Wagemaker and F. M. Mulder, *Solid State Ionics*, 2002, 152, 143-153.

23. M. Kunduraci and G. G. Amatucci, *J Electrochem Soc*, 2006, 153, A1345-A1352.
24. Y. S. Lee, Y. K. Sun and K. S. Nahm, *Solid State Ionics*, 1998, 109, 285-294.
25. H. F. Luo, P. Nie, L. F. Shen, H. S. Li, H. F. Deng, Y. Y. Zhu and X. G. Zhang, *Chemelectrochem*, 2015, 2, 127-133.
26. X. G. Hao, M. H. Austin and B. M. Bartlett, *Dalton T*, 2012, 41, 8067-8076.
27. J. H. Lee, J. K. Hong, D. H. Jang, Y. K. Sun and S. M. Oh, *J Power Sources*, 2000, 89, 7-14.
28. N. Amdouni, K. Zaghib, F. Gendron, A. Mauger and C. M. Julien, *Ionics*, 2006, 12, 117-126.
29. J. H. Kim, S. T. Myung, C. S. Yoon, S. G. Kang and Y. K. Sun, *Chem Mater*, 2004, 16, 906-914.
30. Q. M. Zhong, A. Bonakdarpour, M. J. Zhang, Y. Gao and J. R. Dahn, *J Electrochem Soc*, 1997, 144, 205-213.
31. J. H. Cho, J. H. Park, M. H. Lee, H. K. Song and S. Y. Lee, *Energ Environ Sci*, 2012, 5, 7124-7131.
32. D. W. Shin, C. A. Bridges, A. Huq, M. P. Paranthaman and A. Manthiram, *Chem Mater*, 2012, 24, 3720-3731.
33. A. Y. Shenouda and H. K. Liu, *J Power Sources*, 2008, 185, 1386-1391.
34. X. Fang, N. Ding, X. Y. Feng, Y. Lu and C. H. Chen, *Electrochim Acta*, 2009, 54, 7471-7475.
35. G. Q. Wang, J. Xie, T. J. Zhu, G. S. Cao, X. B. Zhao and S. C. Zhang, *Funct Mater Lett*, 2014, 7.
36. A. Manthiram, K. Chemelewski and E. S. Lee, *Energ Environ Sci*, 2014, 7, 1339-1350.
37. K. R. Chemelewski and A. Manthiram, *J Phys Chem C*, 2013, 117, 12465-12471.

Graphical Abstract

$\text{Li}_{1+x}\text{Ni}_{0.5-x}\text{Mn}_{1.5}\text{O}_4$, made via a novel one-step co-precipitation route, undergoes a disordered-to-ordered phase change. Transition metal ions in tetrahedral sites could influence performance more than the cationic ordering in octahedral site does.

